Characteristics of the JRA-25 Dataset from the Viewpoint of Global Energetics

Yasushi Watarai[1] and H. L. Tanaka[2]

[1]Faculty of Geo-Environmental Science, Rissho University, Japan

[2]Center for Computational Sciences, University of Tsukuba, Japan

watarai@ris.ac.jp

INTRODUCTION

The Japanese 25-year reanalysis (JRA-25) is an up-to-date dataset produced by the Japan Meteorological Agency (JMA) and the Central Research Institute of Electric Power Industry (CRIEPI). The dataset contains global data, with multiple layers from the surface to the middle stratosphere; it is very useful for the study of various meteorological and climatological phenomena.

In order to diagnose the new reanalysis dataset and improve a future reanalysis, it is essential to examine features of the dataset from a variety of perspectives. Some of the advantages and deficiencies of JRA-25 were reported in connection with the impact of some newly-produced observational data, which was summerized by Onogi et al. (2005, 2007). In this study, we examine the characteristics of global circulation represented by the JRA-25 data, from the viewpoint of global energetics.

DATA

The JRA-25 and two other reanalysis datasets are used in this study. These datasets are the same horizontal grid interval (2.5˚ lon. × 2.5˚ lat.), but different number of vertical levels. The details of datasets are summarized in Table 1.

These datasets include 6-hourly data at 0000, 0600, 1200 and 1800Z. The period analyzed in this study is December to February for 22 years (from 1979/80 to 2000/01). The vertical wind (ω), which is essential for the evaluation of energy conversion, is estimated by the integration of horizontal-wind convergence from the top of the atmosphere:

$$\omega(p) = -\int_0^p \nabla \cdot \mathbf{V} dp, \tag{1}$$

with an assumption that $\omega = 0$ at $p = 0$.

Table 1: Reanalysis datasets used in this study.

Dataset:	Japanese 25-year reanalysis (JRA-25)	NCEP/NCAR reanalysis R1 (NCEP1)	ECMWF 40-year reanalysis (ERA-40)
Organization:	JMA/CRIEPI	NCEP/NCAR	ECMWF
Period:	1979-present	1948-present	1957.9-2002.8
Resolution:	T106L40	T62L28	TL159L60
Horizontal grid:	2.5˚ lon. × 2.5˚ lat.	2.5˚ lon. × 2.5˚ lat.	2.5˚ lon. × 2.5˚ lat.
Vertical levels:	23 levels (1000 – 0.4 hPa)	17 levels (1000 – 10 hPa)	23 levels (1000 – 1 hPa)
Used variables:	horizontal wind (u, v), temperature (T) and dew-point depression (T-T_d)	horizontal wind (u, v), temperature (T) and specific humidity (q)	horizontal wind (u, v), temperature (T) and specific humidity (q)
Reference:	Onogi et al. (2007)	Kalnay et al. (1996)	Uppala et al. (2005)

METHOD

In order to examine general circulation, we use the energy cycle devised by Lorenz (1955) and their expansion by Saltzman (1957, 1970). The energy cycle by Lorenz (1955) consists of available potential energy (P) and kinetic energy (K) equations divided between zonal ($_Z$) and eddy ($_E$) components.

$$\partial P_Z/\partial t = G(P_Z) - R(P_Z,P_E) - C(P_Z,K_Z), \quad (2)$$

$$\partial P_E/\partial t = G(P_E) + R(P_Z,P_E) - C(P_E,K_E), \quad (3)$$

$$\partial K_Z/\partial t = M(K_E,K_Z) + C(P_Z,K_Z) - D(K_Z), \quad (4)$$

$$\partial K_E/\partial t = -M(K_E,K_Z) + C(P_E,K_E) - D(K_E). \quad (5)$$

Here C is the conversion term from P to K. R and M are the zonal-eddy interaction of P and K, respectively. G and D are the generation of P and the dissipation of K, respectively. Saltzman (1957,1970) expanded them into the spectral energetics by the Fourier decomposition in zonal direction. Then, eddy equations (3) and (5) are rewritten as follows:

$$\partial P(n)/\partial t = G(n) + R(n) + S(n) - C(n), \quad (6)$$

$$\partial K(n)/\partial t = -M(n) + L(n) + C(n) - D(n). \quad (7)$$

Here n is the zonal wave number and n = 1, 2, 3, …, N. The maximum zonal wave number estimated by (6) and (7) is N = 72. S and L are the eddy-eddy interaction of P and K, respectively.

RESULTS

Figure 1 shows the global energy cycle for the three reanalysis datasets, estimated by equations (2) – (5). The global energy cycle of JRA-25 is similar to that of the other datasets. However, there are several differences among the datasets in Fig. 1. Characteristic of JRA-25 is to have the largest $C(P_Z,K_Z)$ (about 150% of NCEP1 and ERA-40) and dissipation terms (about 110% for $D(K_Z)$ and about 120% for $D(K_E)$). NCEP1 is the smallest of the three datasets in baroclinic eddy conversion terms. Most components of energy cycle show that ERA-40 is larger than JRA-25 and NCEP1.

Figure 2 shows the spectra of P and K for the zonal wave number (n) domain averaged for 22-year DJFs. Both P and K follow closely a -3 power law from n = 7 to 30. The slope of the spectrum is almost the same among the three datasets for $n \leq 30$. In each zonal wave number, the magnitude of energy is ERA-40 ≥ JRA-25 ≥ NCEP1 on the whole. For high-frequency eddies, the energy level for the NCEP1 decreases compared with the -3 power law for $n \geq 35$, and that of the ERA-40 for $n \geq 60$. On the other hand, the spectrum for the JRA-25 does not have such a rapid decrease, for either P or K.

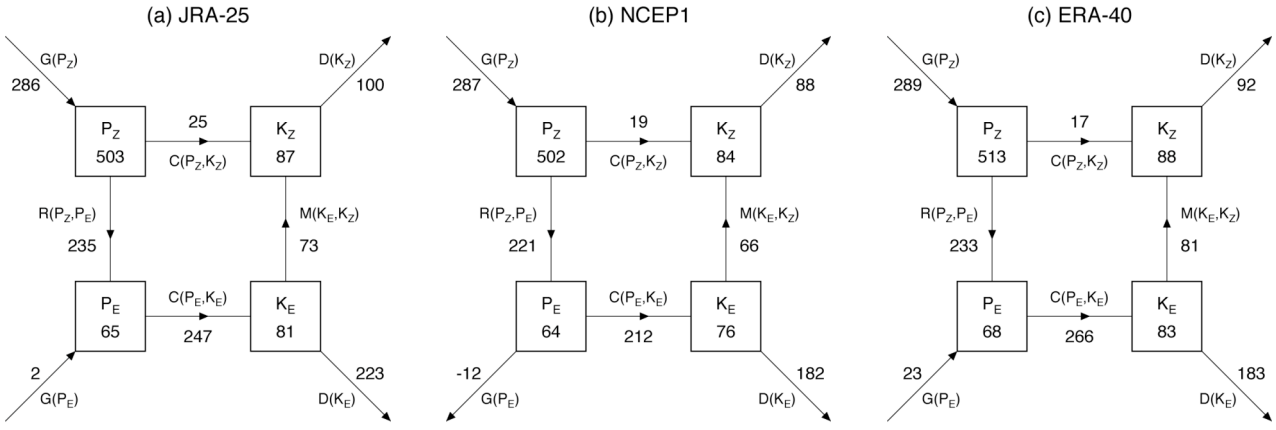

Figure 1: Global energy cycle from (a) JRA-25, (b) NCEP1 and (c) ERA-40 for 22-year DJFs. Generation (G) and dissipation (D) terms are estimated by residuals. Values of the time change terms are omitted. Units are 10^4 Jm^{-2} for energy and 10^{-2} Wm^{-2} for energy conversion.

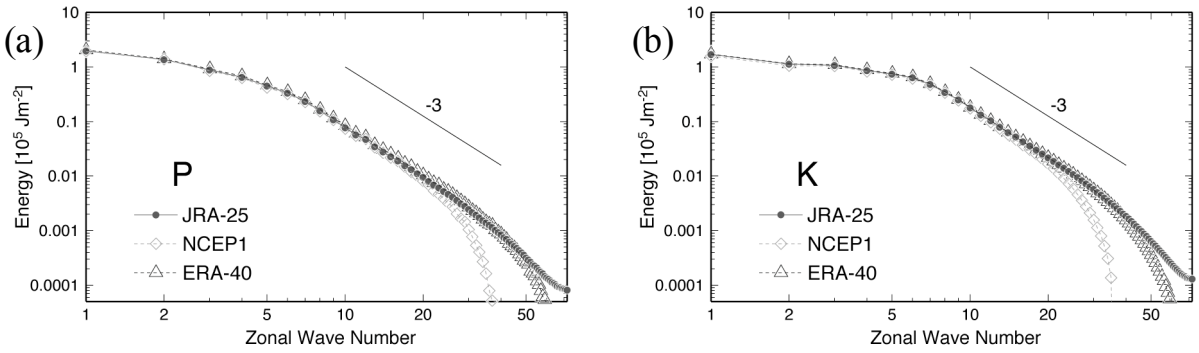

Figure 2: Energy spectra of (a) P and (b) K for 22-year DJFs. Circle, diamond and triangle symbols represent the JRA-25, NCEP1 and ERA-40, respectively. Unit of energy is 10^5 Jm^{-2}.

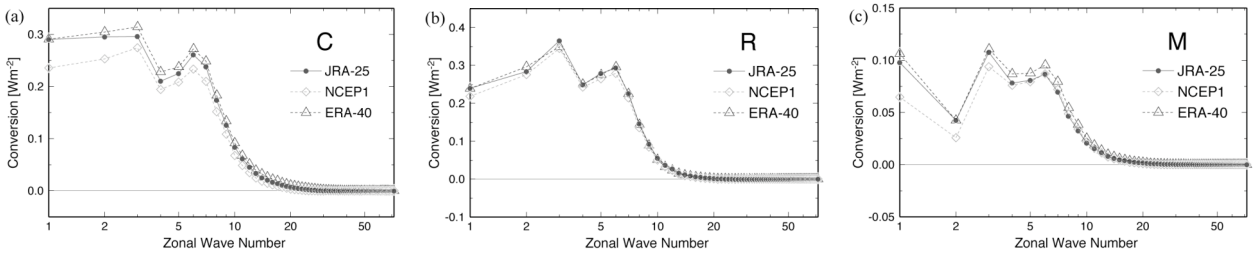

Figure 3: Spectra of (a) baroclinic conversion, $C(n)$, and zonal-eddy interactions of (b) available potential energy, $R(n)$, and (c) kinetic energy, $M(n)$, averaged over 22-year DJFs. Symbols are the same as in Fig. 2.

Saltzman's (1957, 1970) energy cycle allows analyzing the energy and the energy conversion of each zonal wave number of eddies and the interaction between eddies. Figure 3 illustrates the spectra of $C(n)$, $R(n)$ and $M(n)$. Figure 3(a) shows that there are two maxima of $C(n)$ at $n = 3$, which corresponds to the planetary scale, and $n = 6$, which corresponds to the synoptic scale. Among the three datasets, the spectrum is consistent qualitatively, but the conversion at each wave number quantitatively decreases in the following order: ERA-40 > JRA-25 > NCEP1. The magnitude of $R(n)$ is comparable to $C(n)$ in each wave number, which indicates that the inflow by $R(n)$ balances with the outflow by $C(n)$ (Fig. 3b). On the other hand, Fig. 3c displays that the magnitude of $M(n)$ is about one third of $R(n)$ or $C(n)$ for each n. There are two maxima of $R(n)$ or $M(n)$ at $n = 3$ and 6, and the magnitude is ERA-40 > JRA-25 > NCEP1 for each wave number, which is the same as $C(n)$. In addition, it seems that $M(n)$ in JRA-25 is close to that in ERA-40 on the planetary scale ($n = 1$ to 3) and to NCEP1 on the synoptic scale.

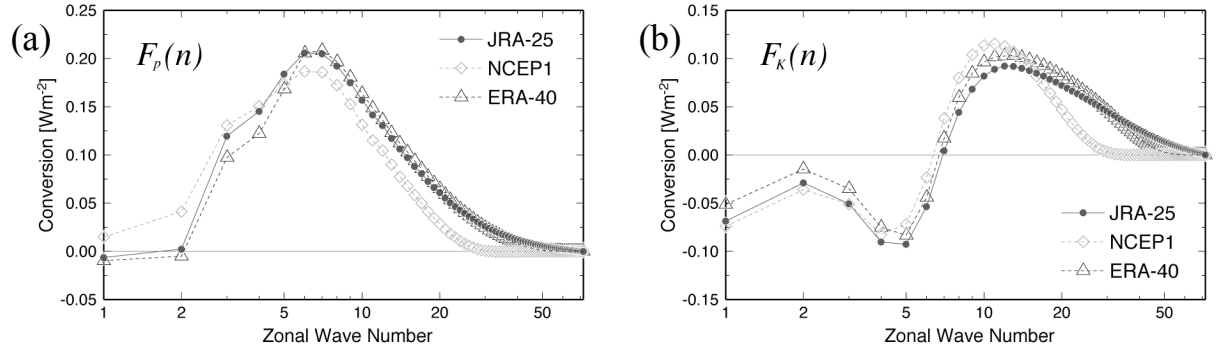

Figure 4: Nonlinear flux functions of (a) available potential energy and (b) kinetic energy for the three reanalysis datasets averaged over 22-year DJFs. Symbols are the same as Fig. 2.

The nonlinear eddy-eddy interactions can be shown more clearly by the flux functins of P and K. According to Hansen and Sutera (1984), the flux function can be written as

$$\partial F_P(n)/\partial n = -S(n), \tag{8}$$

$$\partial F_K(n)/\partial n = -L(n), \tag{9}$$

assuming $F_P(0) = F_K(0) = 0$. Figure 4(a) shows that the value of $F_P(n)$ is positive for almost all wave numbers, which suggests the dominance of energy cascades toward smaller eddies. On the other hand, $F_K(n)$ with n = 6 to 11 has a positive slope, which means the loss of K through eddy-eddy interactions at these wave numbers (Fig. 4b). Therefore, the nonlinear interactions of K form an upscale cascade toward planetary eddies and a downscale cascade toward high-frequency eddies. In both $F_P(n)$ and $F_K(n)$, NCEP1 becomes practically zero at high wave numbers, quite different from JRA-25 or ERA-40, as also shown in Fig. 2.

DJF-mean time series of energy and energy conversion terms are shown in Fig. 5 and 6, respectively. Almost all terms have innegligible interannual variability. Especially, remarkable peaks of K_Z appear in DJF of 1982/83 and 1997/98, and its characteristic is emphasized in Northern Hemisphere. These years correspond to the El Niño. We find that time series of K_E tends to correlate negatively with K_Z. As for energy conversion terms, C_Z has remarkable maxima in the Southern Hemisphere and minima in the Northern Hemisphere in 1982/83 and 1997/98. It suggests the relevance between K_Z, K_E and C_Z. In DJF of 1988/89, which corresponds to the La Niña and the appearance of many blockings in the Northern Hemisphere, K_Z and K_E show a minimum and a maximum value, respectively.

In Fig. 5 and 6, the variability of energies and energy conversion terms for the three datasets is broadly similar to each other. However, we can find that there are systematic differences among the three datasets in almost all terms. The difference among them tends to decrease with time. In 1980's, the fact that NCEP1 is smaller than JRA-25 and ERA-40 is remarkable in almost all terms. Especially, this characteristic is found more clearly for eddy components in the Southern Hemisphere.

CONCLUDING REMARKS

In this study, the global energetics represented by JRA-25 was examined for 22-year DJFs from 1979/80 to 2000/01, in comparison with two other reanalysis datasets (NCEP1 and ERA-40). The global energy cycle of JRA-25 is generally consistent with those of NCEP1 and ERA-40. The peaks and slopes of the spectra agree with each other. For example, the spectrum of $C(n)$ shows the same maxima of n = 3 and 6 for the three datasets.

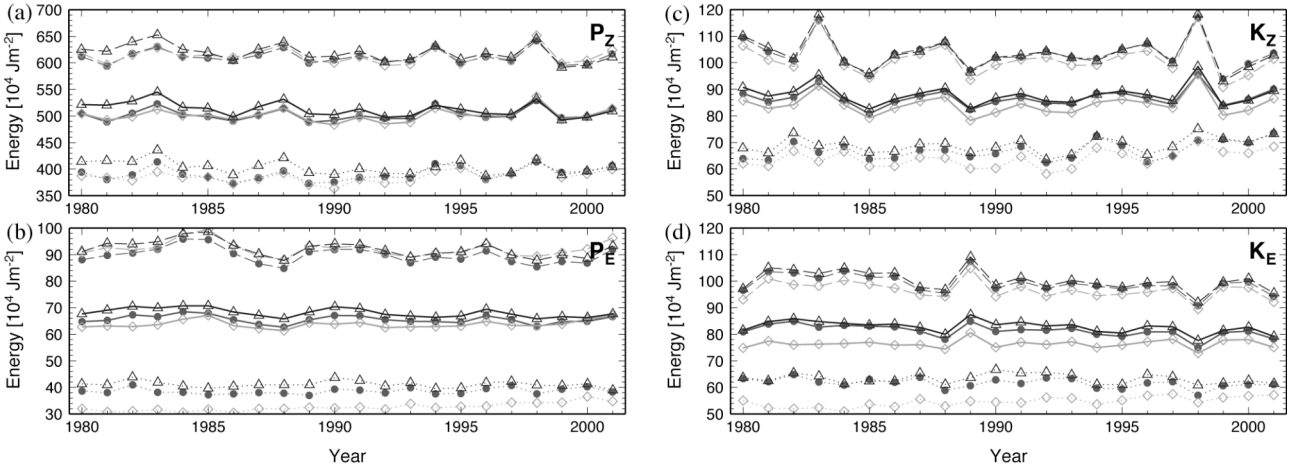

Figure 5: Time series of DJF-mean energy terms: (a) P_Z, (b) P_E, (c) K_Z and (d) K_E. Symbols are the same as Fig. 2. Solid, broken and dotted lines are values averaged over the global, the Northern Hemisphere and the Southern Hemisphere, respectively. Unit of energy is 10^4 Jm^{-2}.

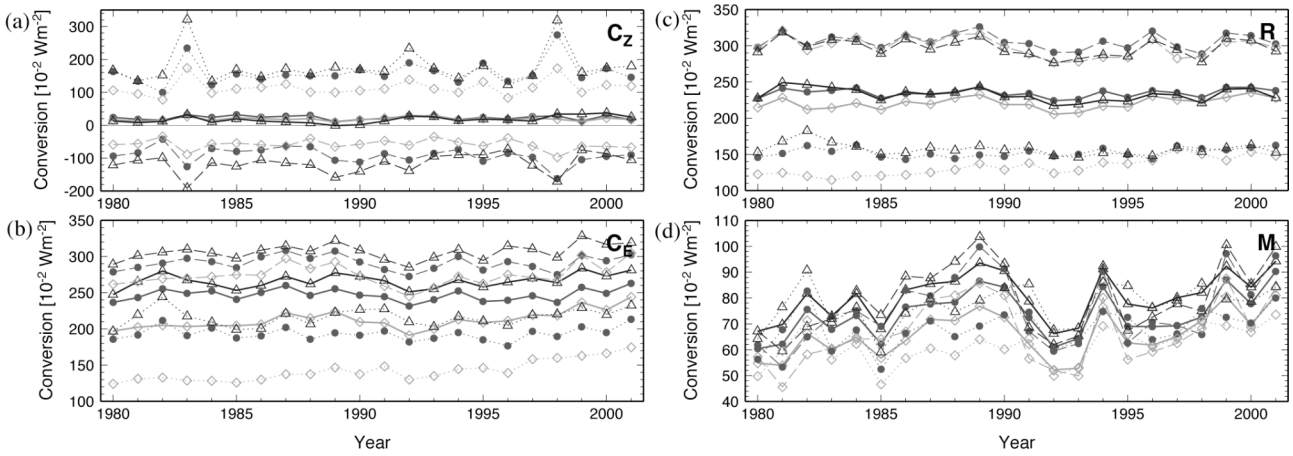

Figure 6: Time series of DJF-mean energy conversion terms: (a) C_Z, (b) C_E, (c) R and (d) M. Symbols are the same as Fig. 2. Solid, broken and dotted lines are values averaged over the global, the Northern Hemisphere and the Southern Hemisphere, respectively. Unit of energy conversion is 10^{-2} Wm^{-2}.

However, the magnitude of energy or energy conversion for each wave number is rather different among the three datasets. Most components of the energy cycle show ERA-40 > JRA-25 > NCEP1. For high-frequency eddies, the energy spectrum for NCEP1 shows a rapid decrease at n = 35. This seems to be the influence of the filtering for released dataset and the model resolution. The decrease in NCEP1 is noticeable at wave numbers as low as $n \sim 20$, which suggests a warning for ≤ 1000-km-scale phenomena in using the NCEP1. On the other hand, JRA-25 does not have such a decrease.

The Lorenz energy cycle (Fig. 1) indicates the relationship of JRA-25 > ERA-40 ~ NCEP1 for C_Z, which is brought about a zonal-mean meridional circulation. There is a dominant Hadley cell in the tropics for all three datasets, which ascends in the area ranged from 5˚S to the equator and descends in 15˚N ~ 30˚N. The magnitude of the circulation shows the relationship of ERA-40 > JRA-25 > NCEP1 (figure not shown). We find that the local value of C_Z is dominant in the Hadley cell, and tends to be positive for ascending wind and negative for descending wind. The disagreement between the magnitude of C_Z and the Hadley cell, therefore, seems to be the result of a large cancellation in the cell. The relationship between the local C_Z and the circulation suggests that the difference between C_Z averaged in the Southern Hemisphere and in the Northern Hemisphere represents the magnitude of the Hadley cell. Time series of C_Z in Fig. 6(a) indicates that the Hadley circulation becomes stronger in the El Niño year.

According to Fig. 5 and 6, the relationship of ERA-40 > JRA-25 > NCEP1 for most components in Fig. 2 is more intense in 1980's than in 1990's. The fact indicates that the time series of the reanalysis data might include in a 'false' trend. Therefore, the trend analysis using a reanalysis dataset should be performed carefully.

REFERENCES

Hansen, A. R. and A. Sutera 1984: A comparison of the spectral energy and enstrophy budgets of blocking versus nonblocking periods. *Tellus*, **36A**, 52-63.

Kalnay, E., M. Kanamitsu, R. Kistler, W. Collins, D. Deaven, L. Gandin, M. Iredell, S. Saha, G. White, J. Woollen, Y. Zhu, M. Chelliah, W. Ebisuzaki, W. Higgins, J. Janowiak, K. C. Mo, C. Ropelewski, J. Wang, A. Leetmaa, R. Reynolds, R. Jenne and D. Joseph 1996: The NCEP/NCAR 40-year reanalysis project. *Bull. Amer. Meteor. Soc.*, **77**, 437-471.

Lorenz, E. N. 1955: Available potential energy and the maintenance of the general circulation. *Tellus*, **7**, 157-167.

Onogi, K., H. Koide, M. Sakamoto, S. Kobayashi, J. Tsutsui, H. Hatsushika, T. Matsumoto, N. Yamazaki, H.

Kamahori, K. Takahashi, K. Kato, R. Oyama, T. Ose, S. Kadokura and K. Wada 2005: JRA-25: Japanese 25-year reanalysis project – progress and status. *Quart. J. Roy. Meteor. Soc.*, **131**, 3259-3268.

Onogi, K., J. Tsutsui, H. Koide, M. Sakamoto, S. Kobayashi, H. Hatsushika, T. Matsumoto, N. Yamazaki, H. Kamahori, K. Takahashi, S. Kadokura, K. Wada, K. Kato, R. Oyama, T. Ose, N. Mannoji and R. Taira 2007: The JRA-25 reanalysis. *J. Meteor. Soc. Japan*, **85**, 369-432.

Saltzman, B. 1957: Equations governing the energetics of the larger scales of atmospheric turbulence in the domain of wave number. *J. Meteor.*, **14**, 513-523.

Saltzman, B. 1970: Large-scale atmospheric energetics in the wave-number domain. *Rev. Geophys. Space Phys.*, **8**, 289-302.

Uppala, S. M., P. W. Kållberg, A. J. Simmons, U. Andrae, V. da Costa Bechtold, M. Fiorino, J. K. Gibson, J. Haseler, A. Hernandez, G. A. Kelly, X. Li, K. Onogi, S. Saarinen, N. Sokka, R. P. Allan, E. Andersson, K. Arpe, M. A. Balmaseda, A. C. M. Beljaars, L. van de Berg, J. Bidlot, N. Bormann, S. Caires, F. Chevallier, A. Dethof, M. Dragosavac, M. Fisher, M. Fuentes, S. Hagemann, E. Hólm, B. J. Hoskins, L. Isaksen, P. A. E. M. Janssen, R. Jenne, A. P. McNally, J.-F. Mahfouf, J.-J. Morcrette, N. A. Rayner, R. W. Saunders, P. Simon, A. Sterl, K. E. Trenberth, A. Untch, D. Vasiljevic, P. Viterbo and J. Woollen 2005: The ERA-40 reanalysis. *Quart. J. Roy. Meteor. Soc.*, **131**, 2961-3012.